Investigating the mesoscale impact of artificial reservoirs on frequency of rain during growing season

Ahmed M. Degu[1] and Faisal Hossain[1]

Received 24 May 2011; revised 13 March 2012; accepted 21 March 2012; published XX Month 2012.

[1] The specific question that this study pursued is "*Have large dams modified the downwind frequency of rainfall in the mesoscale during growing season?*" Rigorously quality controlled precipitation data comprising 3055 stations from the Global Historical Climatology Network (GHCN) were analyzed with 92 large dams in the U.S. Using 30 years of atmospheric reanalysis data, the wind rose diagram for each dam was derived from wind data at the 850 mb level. Around 96 (78) GHCN downwind (upwind) precipitation stations were identified that were within 100 km (mesoscale) of dams. The Mediterranean and humid subtropical climates were found to have experienced the highest and statistically significant change in trend in precipitation frequency downwind and within 100 km of dams during the growing season. The warm summer continental climatic region was found to have exhibited the next most modification. Paired analyses were performed as a function of predam and postdam and at upwind and downwind locations. For Mediterranean climates, the stations studied were found to have experienced a generally weak trend in precipitation frequency before the construction of the selected dams and a systematically more impacted trend during the postdam period. However, using precipitation observations alone, the specific role played by irrigation dams could not be distinguished from other types of dams in this study. Analysis of humidity records, however, revealed that dams can increase the moistening of the air mass by about 5%–15% (in terms of vapor pressure) as it passes downwind, while the effect can also be marginal for other dams. In summary, our study reveals that it is easier to establish a physically intuitive connection between large dams and downwind frequency of rain, but it is much more difficult to demonstrate this connection consistently for all the downwind stations in the mesoscale without the use of additional geophysical data (e.g., topography, land use, and land cover patterns) and mesoscale atmospheric modeling.

Citation: Degu, A. M., and F. Hossain (2012), Investigating the mesoscale impact of artificial reservoirs on frequency of rain during growing season, *Water Resour. Res.*, *48*, XXXXXX, doi:10.1029/2011WR010966.

1. Introduction

[2] The terrestrial water cycle is important for any study that concerns future water availability. There is a large amount of observational and model analyses published in literature that stress the need to improve our understanding of how the extremes of climate and water availability are changing. Of the many important factors, land use and land cover (LULC) change represents a major human-induced activity critical to availability of fresh water [*Chase et al.*, 2000; *Vörösmarty and Sahagian*, 2000; *Hossain et al.*, 2011]. One example of human-induced LULC change is the construction of engineering facilities for irrigation, hydroelectric power generation, and industrial and domestic water supply. In particular, irrigation is one of the major drivers of change in the water cycle. During the last century, irrigable land increased from 40 to 215 Mha [*Freydank and Sieber*, 2008]. About 40% of the current irrigable land is supplied with surface water that is impounded by large artificial reservoirs and dams built on rivers [*Lempérière*, 2006]. Hereafter the term "dam" will be used interchangeably with "artificial reservoir."

[3] Dams can be constructed for different purposes: diversion, irrigation, flood protection, hydropower, water supply, recreation, navigation, etc. The world has approximately 845,000 dams [*Jacquot*, 2009], although an exact number is not yet known. About 50,000 of these can be classified as "large" by the International Commission on Large Dams (ICOLD). The water impounded in these large dams amounts to about 10% of the annual river flow and covers 1/3 of the Earth's natural lake areas [*Jacquot*, 2009]. Though no accurate data is available on the volume of water impounded behind dams, estimates show that up to 10,800 km^3 of water may have been impounded [*Biemans et al.*, 2011]. This volume is equal to a volume of the world's ocean water having a depth of 30 mm [*Chao et al.*, 2008]. Currently the most comprehensive compilation of large dams that describes a wide range of dam properties is

[1]Department of Civil and Environmental Engineering, Tennessee Technological University, Cookeville, Tennessee, USA.

0043-1397/12/2011WR010966

archived by the Global Water Project and is known as the GRanD database [*Lehner et al.*, 2011; *Lehner and Döll*, 2004]. Figure 1 shows the distribution of these large dams digitized in the GranD database around the world along with their main purpose. According to this GranD database, about 34% of these large dams are engaged in irrigation.

[4] Irrigation in the Northern America Great Plains started in the early 1940s and peaked in the 1950s and 1960s mainly due to the construction of large dams during the same period [Figure 1; *Biemans et al.*, 2011]. Because irrigation can be an important driver of LULC change by dams, it is important to understand the combined role of the artificial reservoir and irrigation on the alteration of the water cycle in the mesoscale. *Barnston and Schickedanz* [1984] studied the effect of irrigation on the Texas Panhandle and found that irrigation modifies precipitation patterns when a low convergence and uplift condition exists in the vicinity for the moisture to rise to the cloud base. In their findings, an increase in precipitation was observed more during June (>20%) than July and August. It was also observed that irrigation lowered the temperature approximately by 2°C during the hot and growing season and by 1°C during the cold season. *Barnston and Schickedanz* [1984] have also showed a possibility of convection in the absence of convergence when they examined the anomalies in temperature and dew point. The changes in precipitation were observed about 65 to 90 km downwind of irrigated land during the month of June. Similar research on the Texas High Plains has shown that an increase of 6%–18% in summer precipitation can occur approximately 90 km downwind of the irrigated area [*Moore and Rojstaczer*, 2002]. A more recent study on the Great Plains by *DeAngelis et al.* [2010] reported an increase in July precipitation by about 15%–30%. This increase was observed mostly downwind and over the eastern part of Ogalla aquifer [*DeAngelis et al.*, 2010]. Hereafter, rainfall is used as shorthand for precipitation.

[5] A statistical analysis of observed rainfall downwind of irrigated land in south Spain (upper and lower Vegas and lower Guadalquivir) found a significant increase in mean rainfall, ratio of monthly precipitation to annual precipitation, and number of months with minimum precipitation after irrigation when compared with pre-irrigation records [*Jodar et al.*, 2010]. In general, the simplest physical explanation for the increase in precipitation (frequency and magnitude) due to irrigation that is afforded from literature is as follows. Irrigation makes available more surface water for evaporation and transpiration, which can consequently trigger the formation of convective storm systems under the right set of supporting conditions.

[6] In the documented research on the effect of irrigation on precipitation, the specific role of dams has remained largely unexplored. Because irrigation can be one of the major applications of large dams (Figure 1), it is important to understand the role that irrigation (or nonirrigation) dams play on precipitation modification. *Do large irrigation dams have a significantly larger impact downwind of the dam compared to those that are nonirrigation dams? How does this effect compare to those regions that are upwind of the dam or in different climates/seasons?* These are some of the questions worth pursuing for the water management community as new dams continue to be built in the developing world and existing dams continue to age. Downwind of a dam does not necessarily imply it is downwind of the irrigated area. However, any noticeable effect observed downwind of an irrigation dam may support the notion that the open body of water that is available for direct evaporation during the growing season may modify the pre-existing precipitation process. A large part of the observed increase in precipitation reported in published literature may also be due to a modification of precipitation frequency [*Groisman et al.*, 1999; 2005]. Thus, it is important to understand how dams (irrigation or otherwise) have impacted the frequency of rainfall in the mesoscale (within 100 km) along the downwind direction.

[7] In order to study the impact of large dams on frequency of rain, particularly for those that are engaged in irrigation, it makes logical sense to focus on the growing

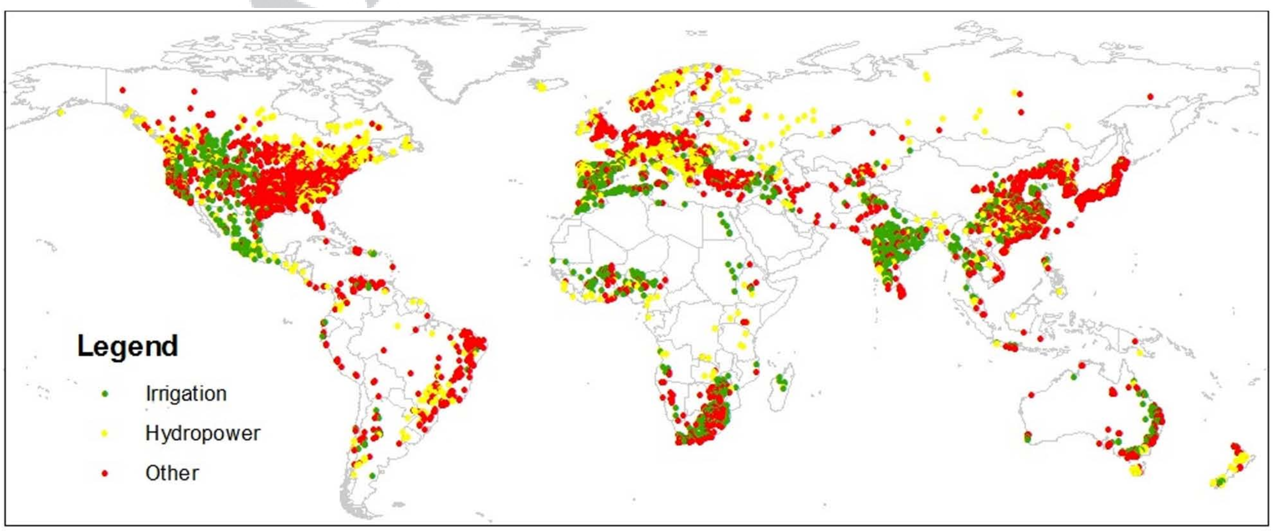

Figure 1. Global distribution of GranD large dams and their main purpose [*Lehner et al.*, 2011].

season. The growing season in North America typically represents the period spanning from April to September when irrigation is in full swing, resulting in intense evapotranspiration and moisture availability. During the growing season, the mesoscale impact of LULC change can be expected to dominate, particularly for those regions with no underlying and larger-scale meteorological process (such as the monsoon system). We recognize that the exclusive focus on the growing season is associated with some key assumptions and limitations. These are discussed later in section.2.

[8] A recent study by *Degu et al.* [2011] showed that large dams significantly modify convective available potential energy (CAPE) in the local surrounding and creates strong spatial gradients for regions in the Mediterranean and arid climates. Because CAPE is one of main ingredients of convective rainfall during the growing season, it is plausible to expect that large dams may also intensify the frequency of heavy rain at downwind locations under certain circumstances. The specific science question that this study pursues is, therefore, "*Have large dams impacted the downwind frequency of rainfall in the mesoscale during the growing season?*" This is achieved by studying a large set of dams located in North America juxtaposed with climatologic wind analysis and precipitation records spanning several decades into predam and postdam periods.

2. Data and Methodology

[9] Ninety-two (92) dams classified as large, according to the ICOLD and located in the U.S., were selected for the study. The geospatial aspect of the data on dams was documented and made available through the Global Water Systems Project (GWSP) Digital Water Atlas [*GWSP*, 2008]. The location of these dams along with the surrounding climate is shown in Figure 2a (upper panel). The climate class is according to the Koppen-Geiger system [*Peel et al.*, 2007]. To identify the potential effect of irrigation dams, the main purpose of each dam was also identified as belonging to one of three broad categories: "irrigation," "hydropower," and "other" (Figure 2a, upper panel). Here "other" refers to applications comprising some or all of the following: flood control, domestic water supply, and recreation.

[10] In order to establish the prevalent wind direction at a seasonal time scale, wind velocity data at the pressure level of 850 mb was used. This data pertained to the National Center for Environmental Prediction (NCEP) North American Regional Reanalysis (NARR) data set [*Mesinger et al.*, 2006]. The wind data was available at a resolution of 32 km over a period spanning 1979 to 2010 (~30 years). The choice of the height (or pressure level) to compute the precipitation-relevant wind direction may be somewhat subjective. While the height should be inclusive of the prevalent cloud base height, various researchers have used different pressure levels for their downwind analysis. For example, *DeAngelis et al.* [2010] used wind velocity at 850 mb level to investigate the effect of irrigation on precipitation in the Great Plains. *Shepherd et al.* [2002] chose 700 mb for exploring the rainfall modification by urban areas. In this study we have chosen 850 mb because of our focus on the growing season (April–September) to adequately account for low-lying and tall cumulus clouds that are quite widespread during the growing season.

[11] The prevalent wind direction was calculated in the form of a standard wind rose diagram from the two horizontal wind velocity vectors (u and v) available at daily time step. Figure 3 shows an example for four dams located at different regions of the U.S. The radial direction represents the axis quantifying the frequency of occurrence along a certain geographic direction (computed as a 30 year climatologic average). The color represents the intensity of the wind speed along that direction. The daily directional data were averaged depending on the season of interest. In this study, wind direction during the growing season (April–September) was of interest. Consistent with the wind rose diagrams, precipitation observation pertaining to the same growing season of each year was also used for computing the frequency trend. Hereafter, therefore, precipitation frequency for a given year refers to the number of days with rain (exceeding a given threshold) during the six months of the growing season from April to September. However, it should be noted that the exclusive focus on the growing season naturally leads to some limitations. For example, in many regions of the U.S., such as in California, most of the precipitation occurs during the cool (winter) season and not during the growing season. Thus, such regions may not exhibit a strong impact during the growing season. Our study is, nevertheless, consistent with the underlying testable hypothesis that large dams impact precipitation frequency downwind during the growing season.

[12] Daily precipitation data were obtained from the Global Historical Climate Network (GHCN), which is available from the National Climate Data Center (NCDC) on the website http://www.ncdc.noaa.gov/oa/climate/ghcn-daily/. The precipitation record archived by GHCN is collected from different sources and merged for quality control. In this study the precipitation data set was extracted for numerous stations in the United States. After a comprehensive quality assessment, only those stations with more than 30 years of continuous and reliable measurement were retained for analysis. Herein, "continuous" refers to a data record having less than 10% of missing data and no more than three straight years of an observation gap. Such a quality requirement resulted in a set of 3055 high quality precipitation stations for analysis (for their location, see Figure 2a, bottom panel). For each station, the number of days with rainfall exceeding a given threshold was computed for each year (hereafter called annual "precipitation frequency" in units of "days/year"). The thresholds considered were: of 1, 5, 10, and 15 mm day^{-1}. The purpose of computing the annual frequency of rain as a function of an increasing threshold was to understand the effect of dams on heavier rainfall that is typical during the growing season due to cumulus convection.

[13] To achieve the study goals of attributing a modification (increase or decrease from the long-term mean trend) in rainfall frequency to the nearby dam, we adopted a step-by-step approach summarized in Figure 4. This approach had the following major steps to arrive at a robust set of upwind and downwind "frequency impacted" and statistically significant stations within 100 km of a large dam:

[14] 1. The time series of rainfall frequency (during growing season) for all the 3055 quality controlled GHCN stations was calculated.

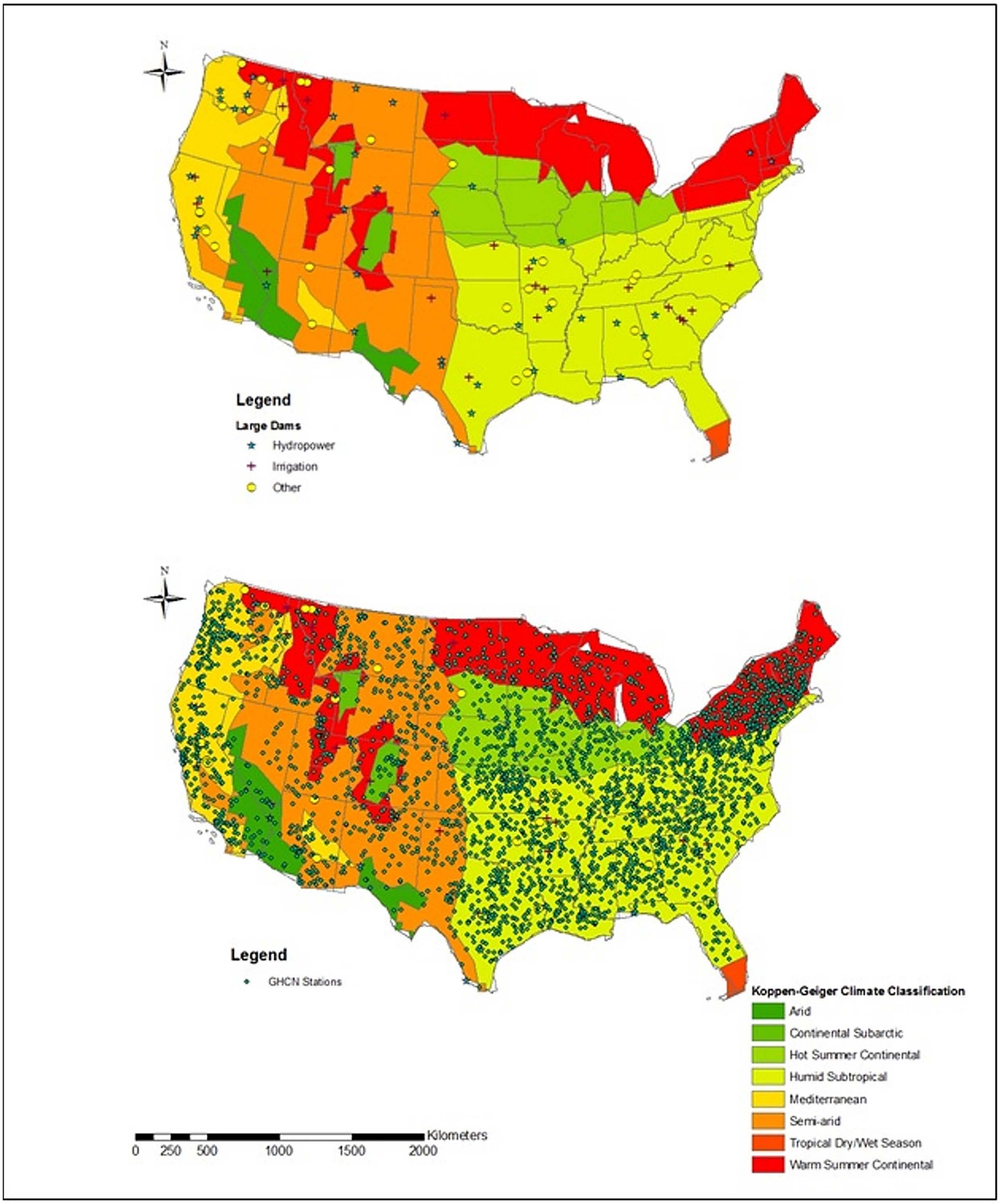

Figure 2. (a) Upper panel: Location of the 92 large dams used in the study. Each colored region represents a climate zone according to the Koppen-Geiger classification. Symbols indicate the main purpose of the dam. Lower panel: Location of 3055 GHCN stations used for precipitation frequency analysis. (b) GHCN stations with positive and negative slopes in rainfall frequency time series (using threshold of 1 mm day^{-1}) according to the least-squares linear fit.

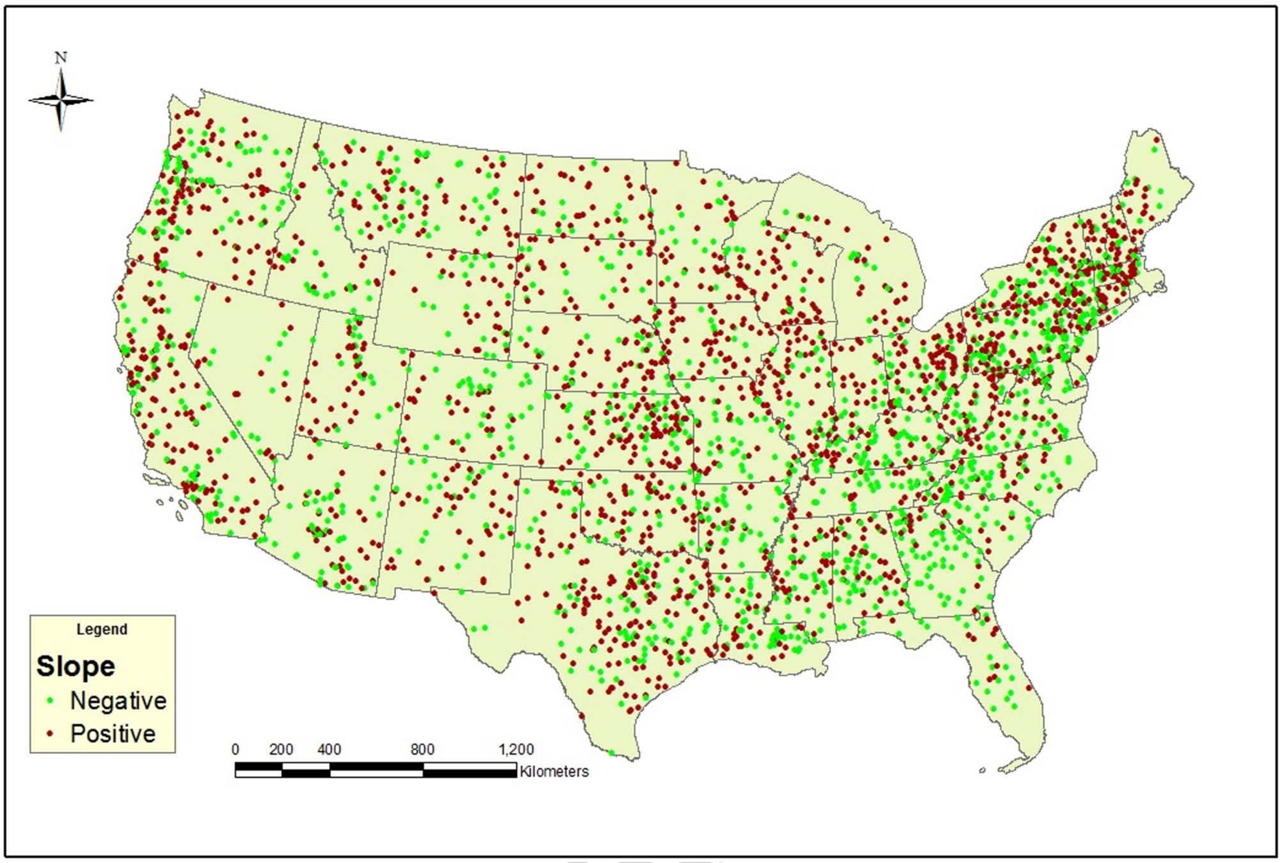

Figure 2. (continued)

[15] 2. Each time series was then fitted with a linear trend line using the method of least squares (Figure 2b provides the map of stations with positive and negatives slopes according to this method for a threshold of 1 mm day^{-1}).

[16] 3. Test for normality of residuals (i.e., the difference between predicted frequency from fitted line and observed frequency) was performed. Sen's slope was also computed for each trend line to filter out any station with a prevalence of outlier data (Table 1). Stations that did not pass the test for normality of residuals or Sen's slope were discarded.

[17] 4. (a) Each least-squares fitted trend line was then tested for significance using the nonparametric methods of *t* test and Mann–Kendall test. This step helped identify only those stations that reported a statistically significant and modified trend (i.e., positive or negative slope of the trend line) at the 95% confidence level (Table 2a).

[18] (b) Each least-squares fitted trend line was subject to a Monte Carlo test proposed by *Morin* [2011] for checking for type II errors that can potentially mask an underlying (increasing or decreasing) trend (described later) (Table 2b).

[19] 5. From step 4 the set of stations with statistically significant and modified (impacted) trend and also within 100 km upwind or downwind of a large dam, was identified for further attribution analysis.

[20] The set of acceptable GHCN stations narrowed down significantly after step 4 of our step-by-step approach with systematic rejection of stations due to filtering out by various tests. For example, more than 80% of the 3055 GHCN stations passed the normality of residuals test, and, hence, the remaining stations (less than 20%) were rejected from the main set during step 3 above (Figure 4). Sen's slope was also computed in this step to reject spurious stations (among the 80% that passed the normality test) impacted by outliers. The Sen's slope is a nonparametric alternative for estimating a slope for a univariate time series. In this method the slopes for all the pairs of ordinal time points are computed and then the median of these slopes is used as an estimate of the overall slope. Thus, the Sen's slope is supposed to be insensitive to outliers and can be used to detect if there is a trend in the data that a linear regression model (and its slope) may not clearly indicate. Although very rarely observed in our study, whenever the Sen's slope and the best-fit line had opposing slope signs, the GHCN station in question was rejected as one potentially spurious due to outliers. Table 1 provides Sen's slope for some select GHCN stations (note: only those stations that passed the Sen's slope test and normality test were then subjected to further significance tests outlined in step 4(a) and step 4(b) next).

[21] Table 2a shows the summary of number of stations in each climatic region that passed the significance test at level of 0.05 (95% confidence), 0.1 (90% confidence), 0.15 (85% confidence), and 0.2 (80% confidence). The purpose of using various levels of significance was to demonstrate its sensitivity to the selection of retained sets. Both tests showed that more than 15% of stations have a significant trend with a 95% confidence level, which is what we focused on afterward.

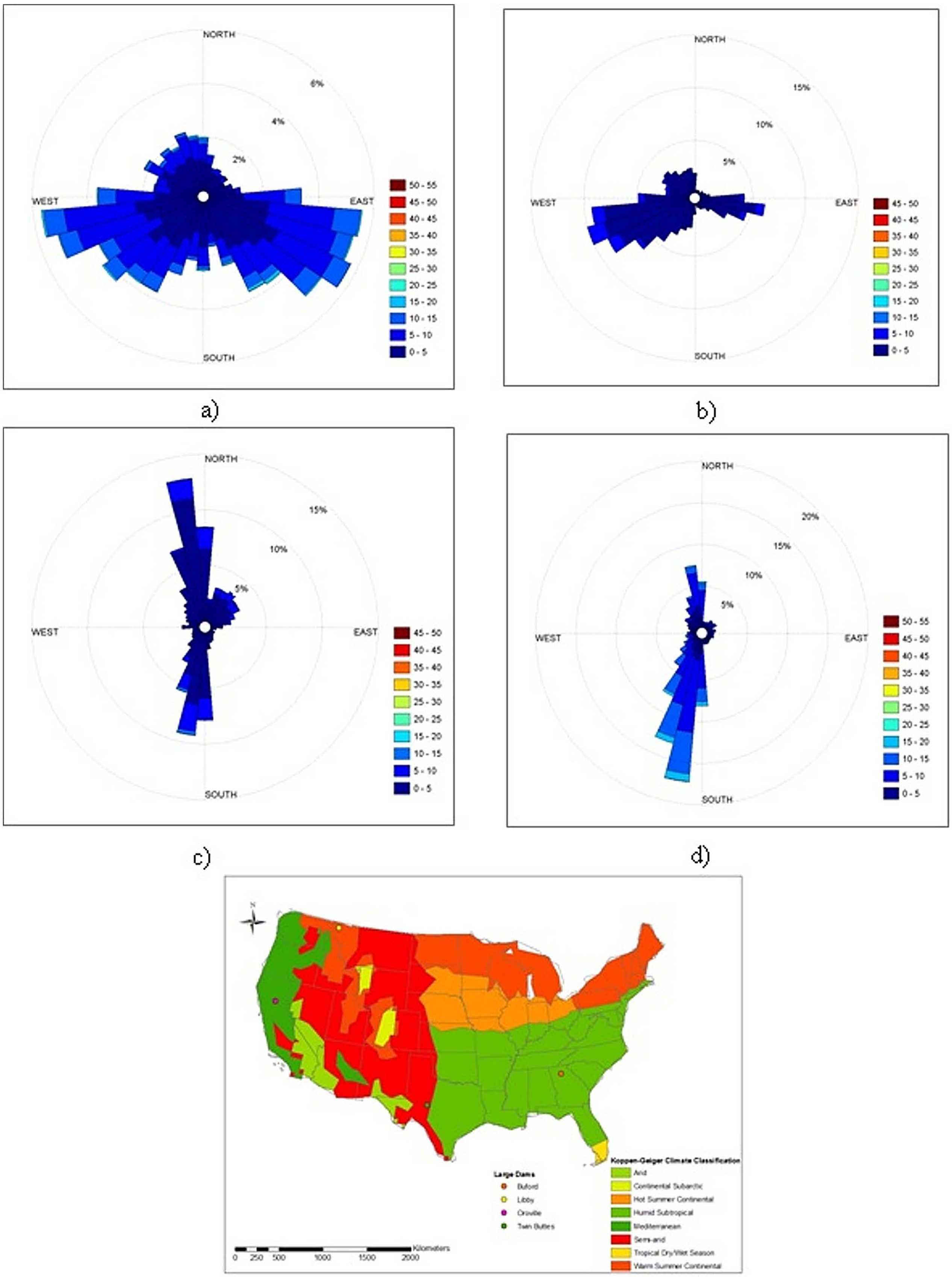

Figure 3. Example of wind rose diagrams for dams named (a) Burford (GA), (b) Libby (MT), (c) Oroville (CA), and (d) Twin Buttes (TX) showing the prevalent wind direction at 850 mb pressure level for the growing season. The center is the dam's spillway. The radial direction represents the axis for frequency of occurrence, while the color represents the average wind speed in m s^{-1}. The location of these dams is shown in (e).

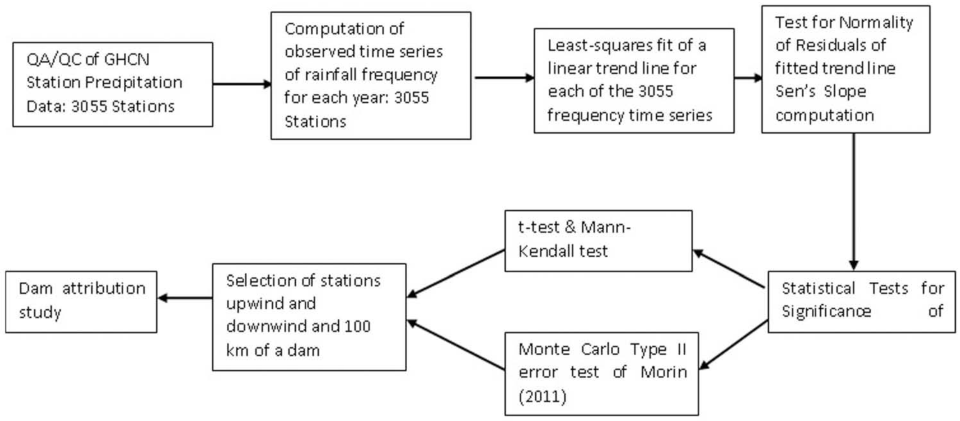

Figure 4. Flowchart showing the step by step approach used to arrive yet at robust set of GHCN stations with statistically significant and modified (impacted) trend and within 100 km of a large dam.

A total of 506 stations (having passed *both* the Mann–Kendall test and the *t* test at 95% confidence level) were thus retained for further consideration. The Monte Carlo test for type II errors of *Morin* [2011] was also performed in this step 4(b).

[22] For the Monte Carlo (MC) test for type II errors, we followed the *Morin* [2011] test that suggests an MC approach of generating numerous but "equiprobable" realization of precipitation frequency trend lines. These equiprobable trend lines were generated by randomly corrupting the best-fit linear trend line by the mean and standard deviation derived from the observed time series of frequency of rainfall. *Morin* [2011] suggests that if more than 50% of these randomly generated trend lines pass a nonparametric test of significance (e.g., *t* test or Mann–Kendall), then the station can be robustly labeled as having marginal type II errors that would otherwise mask a trend. However, *Morin* [2011] also suggested that the significance test be performed for randomly generated trend lines of gradually increasing linear slope to identify the minimum slope at which more than 50% of the MC samples pass the test. In our analysis, 1000 MC realizations of trends were generate for each GHCN station only for one slope pertaining to the actual slope of the best-fit linear line. We observed that only 5%–20% of the randomly generated trend lines per station passed the *t* test (Table 2b). This clearly indicated the high probability (80%) of type II (false negative) errors in the GHCN data that potentially masks an underlying trend. Finally, 96 (78) GHCN downwind (upwind) precipitation stations were identified in step 5 using the step-by-step approach outlined in Figure 4 that satisfied all the four tests (normality of residuals, Sen's slope, nonparametric test, and Morin's test). These stations also satisfied the constraint of being within 100 km of a large dam. These sets of stations were identified from the larger set of GHCN stations exhibiting a statistically significant modification in frequency trends, and, therefore, they include stations that reported a systematic increase or decrease in frequency of rain during the growing season.

Table 1. Comparison of Slopes Obtained From Linear Regression (Least-Squares Fit) and Sen's Slope Method for Select Stations in Various Climate Zones[a]

Climate	GHCN Station	Linear Slope	Sen's Slope
Arid	USC00046197	0.0343	0.0256
	USC00020080	−0.0579	−0.0606
Continental Subarctic	USC00052184	0.0932	0.0889
	USC00050372	−0.3776	−0.4167
Hot Summer Continental	USC00110338	0.0292	0.0337
	USC00118860	−0.1229	−0.1239
Humid Subtropical	USC00011069	0.1413	0.1282
	USC00011301	−0.0492	−0.0328
Mediterranean	USC00023258	0.1569	0.1538
	USC00028904	−0.1964	−0.1667
Semiarid	USC00021059	0.1977	0.1909
	USC00020104	−0.1313	−0.1579
Warm Summer Continental	USC00050130	0.0238	0.0202
	USC00056410	−0.2129	−0.2457

[a]Slope has unit of days per growing season.

3. Results and Discussion

[23] For a first-cut assessment of the general trends, an increase in frequency (i.e., the positive slope of the linear trend line) was observed for about 50% of the 3055 GHCN stations (see also Figure 2b). The average increase in slope for these stations per each climate zone exhibiting an increase is shown in Table 3. It can be inferred from this table that the warm summer continental climate has, in general, experienced the highest increase in rainfall frequency (for threshold >1 mm day^{-1}). The humid subtropical and Mediterranean climatic regions were found to have exhibited the next greatest increase. In an earlier study by *Degu et al.* [2011], large dams located in Mediterranean and semiarid regions were found to exhibit the most distinct patterns of impact in CAPE from multidecadal observational records. This discrepancy may be explained from the fact that most of the precipitation occurs during the winter season for Mediterranean climates, rather than during the growing season. Further analysis breaking down the period as "predam" and "postdam" epochs or as "upwind" and "downwind" of large dams can reveal a clearer picture. This is discussed next.

[24] Figure 5 summarizes the average change in frequency of rain for all the 96 stations located downwind of

Table 2a. Significance Test of GHCN Stations for Modification of Trend in Rainfall Frequency During Growing Season

		Number of Stations Passing the Significance Test Modification of Trends (Negative and Positive Trends)							
		95% Confidence Level		90% Confidence Level		85% Confidence Level		80% Confidence Level	
Climatic Region	Total	*t*-test	Mann–Kendall	*t*-test	Mann–Kendall	*t*-test	Mann–Kendall	*t*-test	Mann–Kendall
Arid	48	4	8	5	8	5	14	9	19
Continental Subarctic	16	3	4	4	4	5	4	7	6
Hot Summer Continental	310	47	108	67	108	83	133	92	151
Humid Subtropical	1290	230	424	323	424	400	509	479	565
Mediterranean	308	28	75	48	75	67	94	82	116
Semiarid	441	66	142	94	142	121	166	141	184
Warm Summer Continental	642	128	249	183	249	231	291	264	324
Total Sum	3055	506	1010	724	1010	912	1211	1074	1365
Percentage (%)		16.56	33.06	23.70	33.06	29.85	39.64	35.16	44.68

Table 2b. Percentage of Monte Carlo Simulated Frequency Time Series Passing the Significance Test at Various Levels of Confidence According to the *t*-Test

		Percentage of the 1000 Monte Carlo Simulated Time Series per Station That Were Found Significant at Given Confidence Level			
Climate	Number of Stations Analyzed	95% Confidence	90% Confidence	85% Confidence	80% Confidence
Arid	48	6.74	12.23	17.60	22.83
Continental Subarctic	16	5.49	10.75	15.73	20.99
Hot Summer Continental	310	5.44	10.64	15.70	20.72
Humid Subtropical	1290	5.52	10.80	15.94	21.00
Mediterranean	308	5.45	10.73	15.89	20.96
Semiarid	441	5.64	10.92	16.08	21.18
Warm Summer Continental	642	5.58	10.83	16.05	21.12

Table 3. Overall Trends in Precipitation frequency Averaged Over Climatic Regions During the Growing Season[a]

	Average Increase (Slope of Linear Trend Line) in Frequency of Rain (Days/Growing Season)			
Climate	Rainfall $\geq$ 1 mm day^{-1}	Rainfall $\geq$ 5 mm day^{-1}	Rainfall $\geq$ 10 mm day^{-1}	Rainfall $\geq$ 15 mm day^{-1}
Arid	0.141	0.074	0.070	0.059
Continental Subarctic	0.084	0.111	0.052	0.045
Hot Summer Continental	0.211	0.157	0.131	0.112
Humid Subtropical	0.215	0.174	0.139	0.117
Mediterranean	0.207	0.141	0.096	0.070
Semiarid	0.183	0.115	0.086	0.066
Warm Summer Continental	0.221	0.146	0.116	0.099

[a]Precipitation frequency is defined in units of "days per growing season" (i.e., six months spanning Apr to Sept). Analysis is presented for those stations, among the 3055 GHCN stations, that experienced an overall increase in precipitation frequency (positive slope in linear trend line according to 1 mm day^{-1} threshold and shown in Figure 2b).

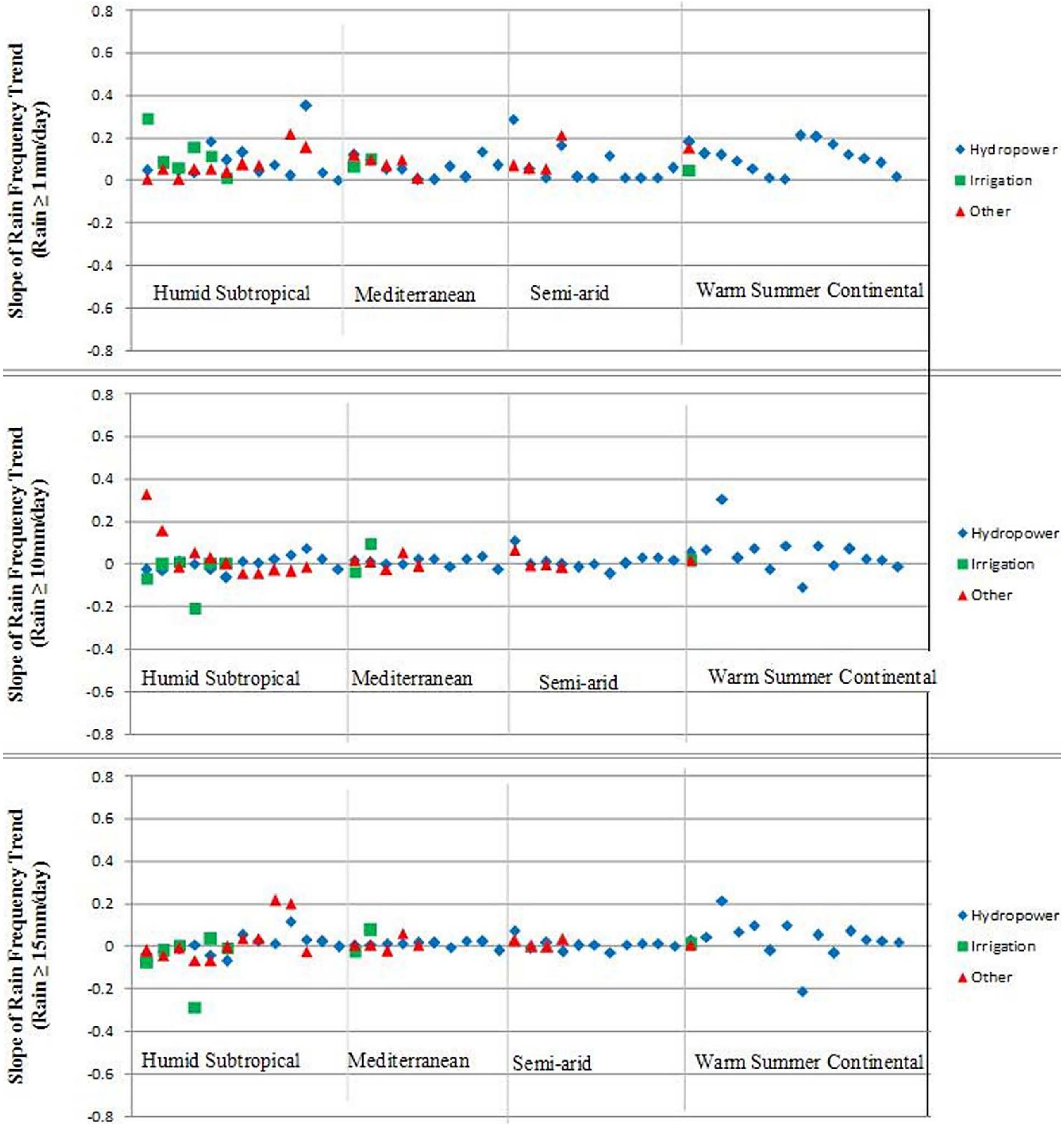

Figure 5. Average change in precipitation frequency during growing season (i.e., slope of the linear trend of the precipitation frequency time series) for the set of GHCN stations that are downwind and 100 km of a dam for three different rainfall thresholds (1 mm day^{-1}—upper panel; 10 mm day^{-1}—middle panel; and 15 mm day^{-1}—lower panel). The color and symbol scheme represents the purpose of the closest dam that a station is downwind to. Only stations pertaining to four major climate zones of the US (humid subtropical, Mediterranean, semiarid and warm summer continental) are shown in the figure.

dams and as a function of climate and rainfall threshold. Here the slope of the best-fit linear trend line fitted to the rainfall frequency time series represents the average increase in frequency in units of days/year. Barring a few exceptions, the impact of most irrigation dams on downwind precipitation frequency is not as clear cut and does not stand out from other types of dams. This is probably due to the fact that downwind of an irrigation dam is not necessarily downwind of the irrigated landscape. The negligible amount of scatter observed in the lower two panels in each climate category shows that the impact of dams on heavier (>10 mm day^{-1}) precipitation frequency probably has not been impacted for heavier rain as much as light rain (<10 mm day^{-1}). Figure 6 shows an example plot of rain frequency trends for a station downwind of the Oroville Dam in California, which is mainly a hydropower dam.

[25] To elucidate a clearer picture on the impact of dams on precipitation frequency, paired analyses were performed as a function of (A) predam and postdam; and (B) at upwind and downwind locations. Figure 7 compares the average change in frequency (during growing season) in terms of pre- and postdam periods for GHCN stations located downwind and within 100 km of a dam. A much more definitive assessment can be made from this figure. For Mediterranean climates, the selected stations experienced a relatively weak trend in precipitation frequency (because of the negative or near-zero slopes) before the construction of a dam within 100 km. The same set of stations experienced a marked change in precipitation frequency as shown by the scatter after the construction of the dam (see lower panel of Figure 7). The same can be concluded for stations near dams located in humid subtropical climates. As an example, Figure 8 shows such a postdam increase from predam in frequency of rainfall for stations near dams located in a Mediterranean climate.

[26] A comparison between the average change in rainfall frequency at downwind and upwind stations for each dam shown in Figure 9 provides additional observational evidence on the mesoscale impact of dams. This comparison is shown for the postdam period using a consistent period of data for both downwind and upwind stations to allow derivation of unbiased estimates. For Mediterranean and semiarid dams, the modification in precipitation frequency downwind of dams appears greater than that at upwind of dams. However, any specific role played by irrigation dams is not distinguishable when wind direction is considered. No clear and distinct differences emerge for other climate regions to arrive at a conclusion that the downwind stations are influenced by dams more than upwind stations in those climates.

[27] To explore if the atmospheric boundary layer can experience moistening as an air mass passes over a reservoir, we also analyzed humidity records at seven weather station locations of NOAA-National Weather Service (NWS) immediately upwind and downwind of three dams in California: (1) Don Pedro Dam; (2) Oroville Dam, and (3) San Luis Dam (Figure 10). The humidity measurements were extracted from a NOAA National Weather Service portal available at http://www.weather.gov/om/osd/portal.shtml. The NWS stations, known more commonly as WBAN (Weather Bureau, Army, Navy) stations, report daily minimum and maximum relative humidity and temperature. We converted the relative humidity observation to vapor pressure units (kPa) in two ways: (1) using daily maximum of relative humidity with minimum daily temperature and (2) using daily minimum of relative humidity with maximum daily temperature. In this way, the minimum and maximum vapor pressure was computed. The

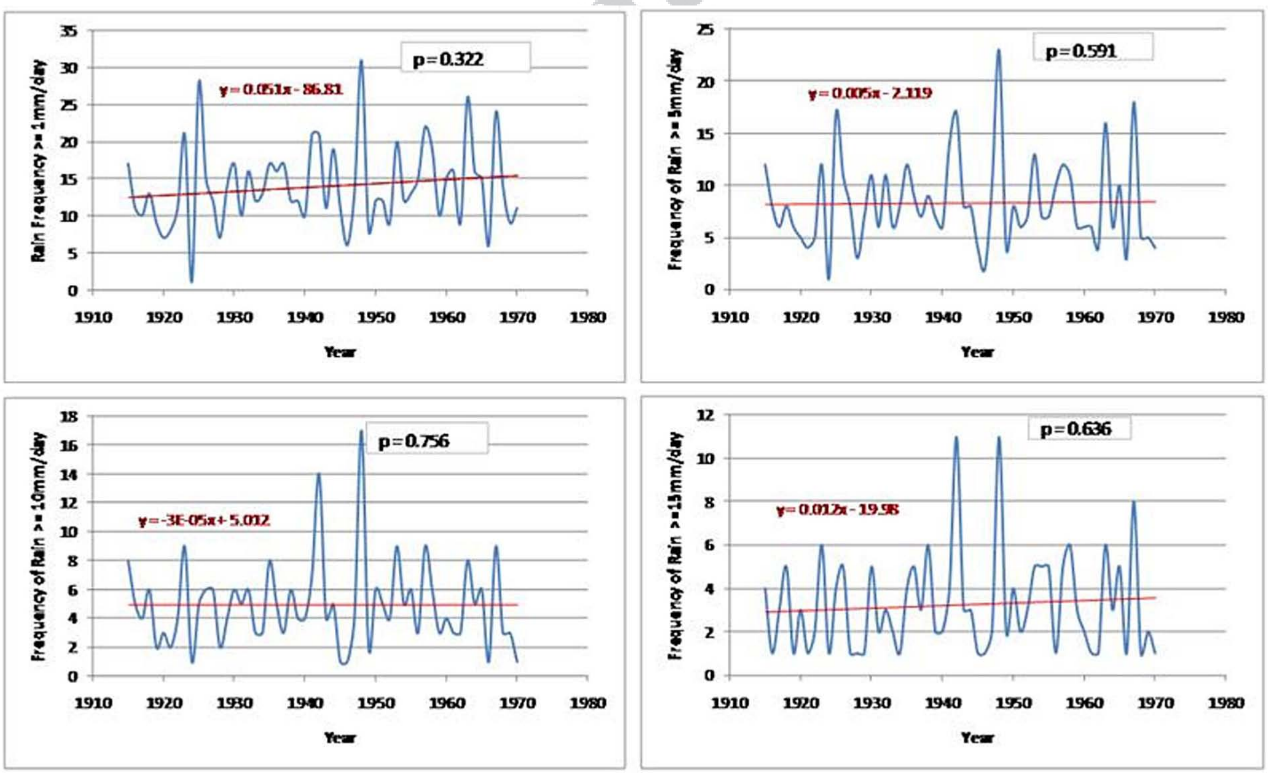

Figure 6. Time series of annual precipitation frequency (days/growing season) for GHCN station USC00041624 located 32.5 km downwind of the Oroville dam in California. Each panel represents a given threshold; 1 mm day^{-1} (upper left); 5 mm day^{-1} (upper right); 10 mm day^{-1} (lower left), and 15 mm day^{-1} (lower right). The p value is provided for each panel.

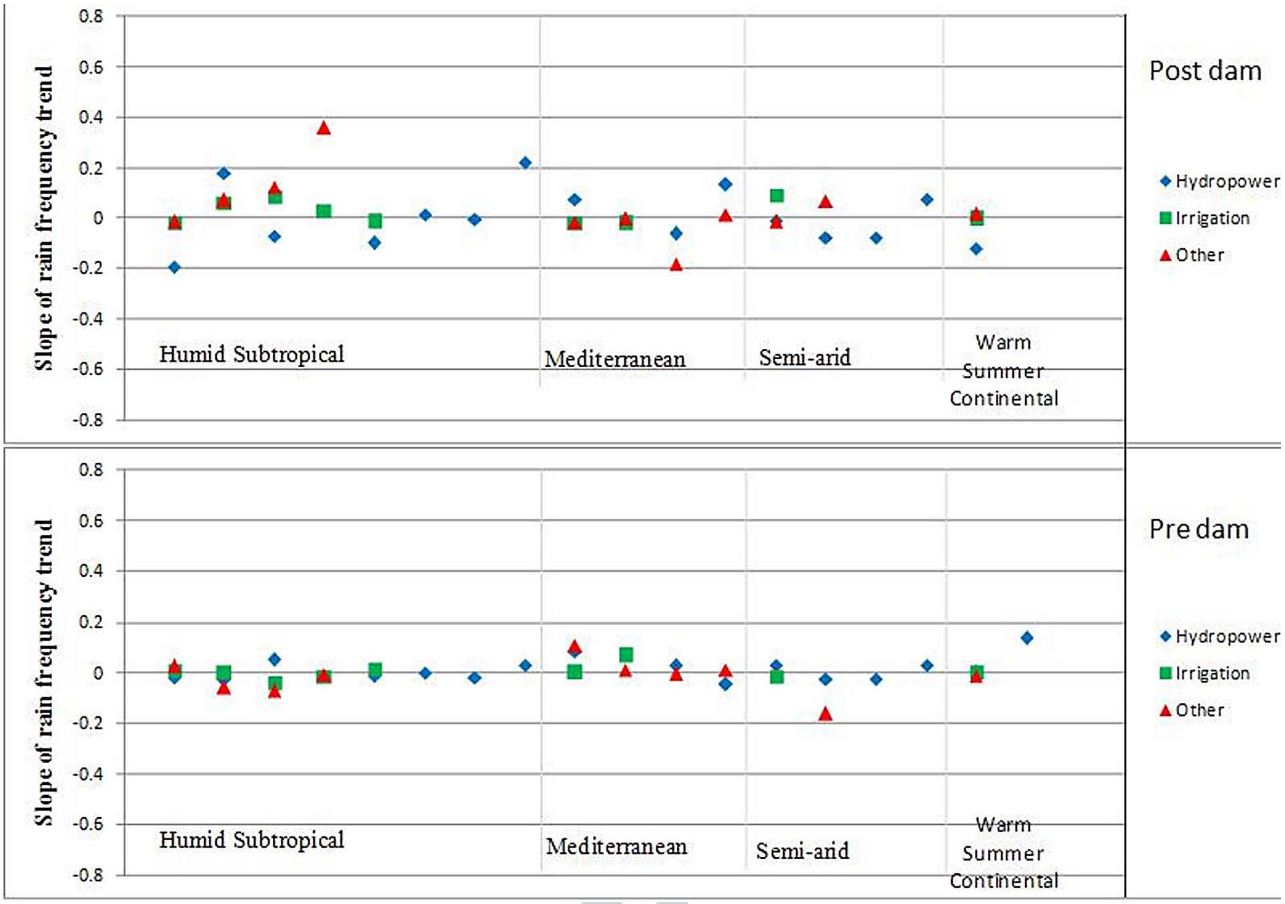

Figure 7. Average change in precipitation frequency (threshold 1 mm day^{-1}) during growing season (i.e., slope of the linear trend line for the precipitation frequency time series) for stations downwind of a dam as a function of predam and postdam periods. The color and symbol scheme represents the main purpose of the closest dam that the station is downwind to. Note: each dam has a specific commission year which divides the period into predam and postdam epochs. Only stations pertaining to four major climate zones of the US (humid subtropical, Mediterranean, semiarid and warm summer continental) are shown in the figure.

daily average for each Julian day was then computed over a period of five recent years. The time series of average minimum and maximum vapor pressure was then compared between stations upwind and downwind to a dam.

[28] An interesting pattern is revealed. Downwind vapor pressure is seen to be consistently and detectably larger than upwind vapor pressure by about 10%–15% for Oroville Dam (Figure 10b), while the difference is marginal for Don Pedro Dam (Figure 10a). For San Luis Dam, the downwind vapor pressure is found to be detectably lower than upwind vapor pressure. It is possible that the growing season wind rose diagram for San Luis Dam is not inclusive of the predominantly southwesterly wind direction during the winter season when most of the vapor transport takes place. The limitations of using the growing season wind rose diagram have been explicitly overviewed earlier in section 2. Overall, the three types of findings point to the need for an atmospheric modeling study involving land use/land cover change dynamics to understand how terrain-induced storms are modified in frequency and magnitude the presence of a large artificial reservoir.

4. Conclusion

[29] The specific question that is pursued is: "*Have large dams impacted the downwind frequency of rainfall in the mesoscale during the growing season?*" Physically it is intuitive to expect an impact on frequency or magnitude in the mesoscale influence zone of a dam if the region is already conducive to convection. With this intuition in mind, we analyzed precipitation stations from the Global Historical Climatology Network (GHCN) with around 92 large dams in the U.S. Using 30 years of atmospheric reanalysis data, the wind rose diagrams for each dam was derived. Around 96 (78) GHCN downwind (upwind) precipitation stations were identified within 100 km of dams. From a large set of 3055 stations, we narrowed down, through a comprehensive step-by-step approach, to a considerably smaller set that exhibited a statistically significant trend in frequency where stations were also located very close to dams. In addition, the fitted time series of frequency were tested for normality of residuals and checked for outliers through the Sen's slope to allow us to make

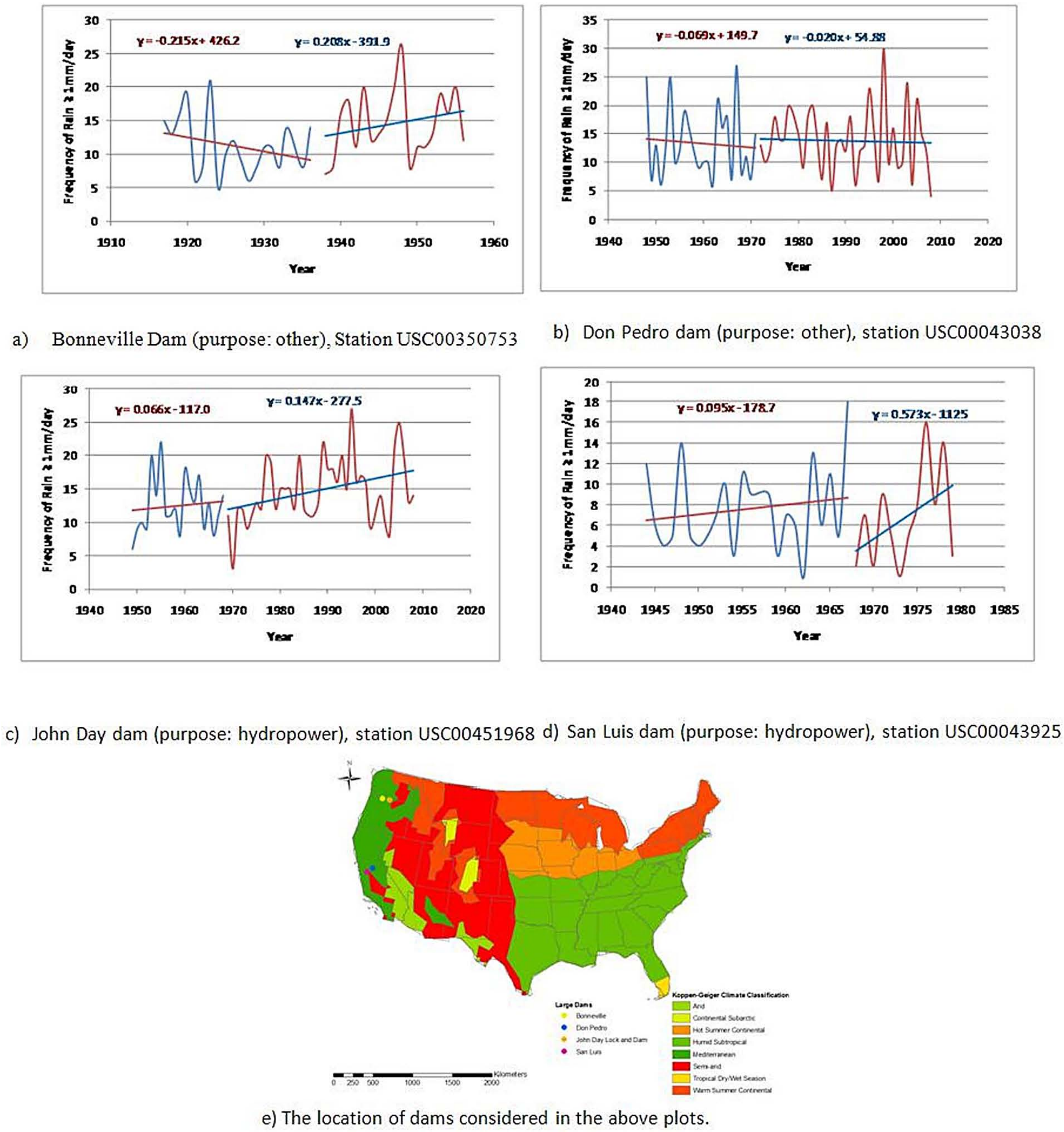

Figure 8. Precipitation frequency time series for predam ("blue" series) and postdam ("red" series) for some stations downwind of dams in Mediterranean regions. Rainfall threshold is 1 mm day^{-1}.

robust attributions. The attribution to dams for neighboring stations experiencing a systematic alteration in frequency was found to follow a nuanced dependence on the specific method of testing for statistical significance. Conventional nonparametric methods (such as *t* and Mann–Kendall tests) revealed statistical significance in the gradually increasing trends in frequency for about 15% of the 3055 stations at the 95% confidence level. On the other hand, a Monte Carlo technique revealed a large percentage (90%) of type II errors in GHCN data that could potentially be masking an underlying trend.

[30] In general, given that about half of the 3055 stations exhibited an increasing trend (Figure 2b), of which only 25% were found to be statistically significant, it appears to us that it is far easier to claim that dams *can* impact frequency of rain than to prove that the dam *has* actually impacted frequency of rain consistently for all nearby downwind stations solely on the basis of precipitation

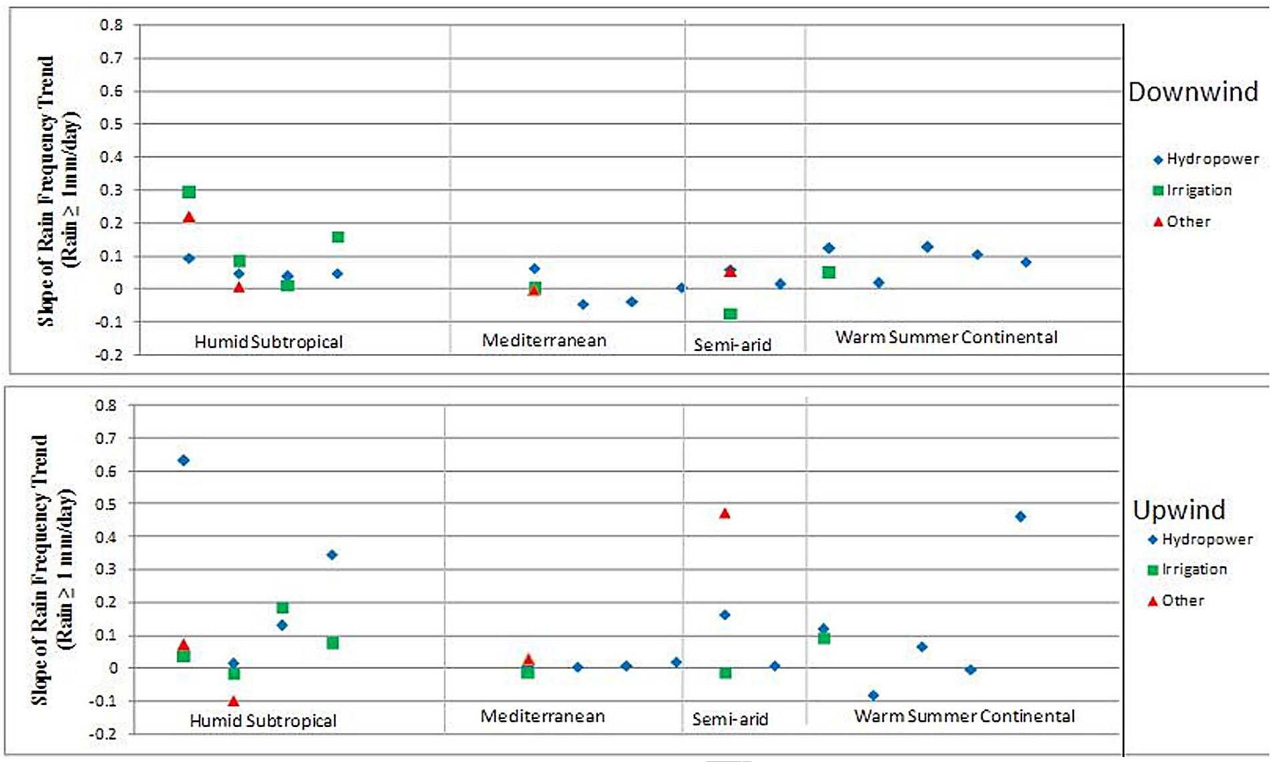

Figure 9. Comparison of the average change in precipitation frequency between downwind and upwind stations. The color and symbol scheme represents the main purpose of the closest dam that the station is downwind and upwind to. Only stations pertaining to four major climate zones of the US (humid subtropical, Mediterranean, semiarid and warm summer continental) are shown in the figure.

observations. This assessment is very similar to the study of peak flows and stationarity by *Villarini et al.* [2009], where the authors state, “Despite the profound changes that have occurred to drainage basins throughout the continental United States and the recognition that elements of the hydrologic cycle are being altered by human-induced climate change, it is easier to proclaim the demise of stationarity of flood peaks than to prove it through analyses of annual flood peak data.”

[31] Barring the statistical nuances, our analysis indicated that the Mediterranean and humid subtropical climates have generally experienced the highest modification in precipitation frequency. The warm summer continental climatic region was found to have exhibited the next highest change. The same two regions have experienced a comparatively higher increase in higher magnitude events (>15 mm day^{-1}) compared to other climates. For Mediterranean climates, a significantly larger number of stations close to the dams were found to have experienced a relatively weak trend in precipitation frequency before the construction of the studied dam and a consistently more modified trend during the postdam period. Our analyses also revealed that the modification in precipitation frequency downwind of selected dams has been greater than that at upwind locations of dams studied for those stations located in humid subtropical and Mediterranean climates. Even though the analysis according to wind direction helped to improve our understanding, the specific role played by irrigation dams could not be distinguished from other dams in this study.

[32] A major motivation of this investigation was premised on the impact of irrigation on precipitation in the downwind regions. Because a significant amount of today’s irrigation water is supplied from large dams, an analysis with respect to the wind conditions relative to a dam is felt worthwhile. However, as mentioned earlier, downwind of an irrigation dam is not necessarily downwind of the irrigated landscape. Our findings have indicated that this issue of impact of irrigation dams requires further investigation by taking into account the spatial orientation of irrigated landscapes [*DeAngelis et al.*, 2010] and chronology of agricultural intensification relative to the location of dams.

[33] Another limitation of our study pertains to our focus on the growing season. A more inclusive study should consider analysis of precipitation frequency trends for the entire year as many climates do not experience significant precipitation during growing season. High resolution satellite rainfall data sets provide an accurate spatiotemporal distribution of rainfall around dams at scales of 25 km and 3 h for specific seasons. Currently, the Tropical Rainfall Measuring Mission (TRMM) multisatellite precipitation analysis [TMPA, *Huffman et al.*, 2010] provides a multiyear global archive of distributed rainfall data (spanning more than 10 years) to perform climatologic analysis. Such data can allow assessment as a function of predam, postdam, and upwind and downwind of a dam and yet have a statistically

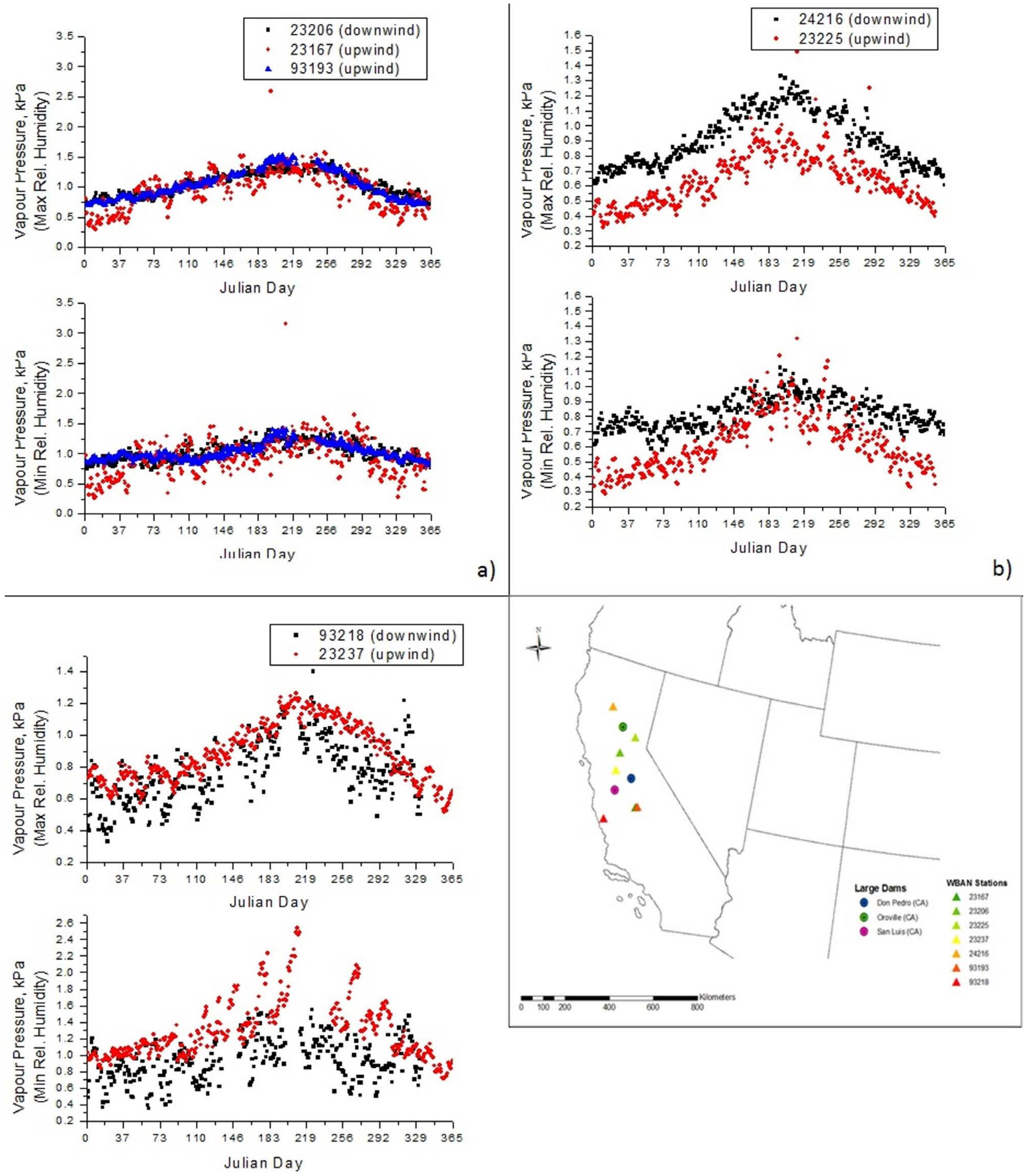

Figure 10. Vapor pressure plot for NWS (WBAN) stations near dams: (a) Stations 02,206, 23,167, and 93,193 located downwind, upwind, and upwind, respectively, of Don Pedro Dam, CA; (b) stations 24,216 and 23,225 located downwind and upwind, respectively, of Oroville Dam, CA; and (c) stations 93,218 and 23,237 downwind and upwind of San Luis dam, CA. Location of stations shown in panel above.

significant sample size to draw inferences on the climatologic frequency of rain around the globe. As a future extension of this study, we plan to include LULC change, particularly irrigation pattern trends, and incorporate the use of satellite precipitation data and other rainfall data sources (such as NOAA's Daily Unified Precipitation) in combination with atmospheric modeling to improve our understanding of the impact of large dams on frequency of rain.

[34] **Acknowledgments.** The first author was supported by a Doctoral Fellowship provided by the Office of Research of TN Technological University through the Southern Regional Education Board. The authors gratefully acknowledge the detailed reviews provided by three anonymous reviewers and the excellent guidance of the Associate Editor that helped to significantly improve the quality of the manuscript.

References

Barnston, A. G., and P. T. Schickedanz (1984), The effect of irrigation on warm season precipitation in the Southern Great Plains. *J. Appl. Meterology Clim*, *23*(6). AQ3

Biemans, H., I. Haddeland, P. Kabat, F. Ludwig, R. W. A. Hutjes, J. Heinke, W. von Bloh, and D. Gerten (2011), Impact of reservoirs on river discharge and irrigation water supply during the 20th century, *Water Resour. Res*, *47*, W03509.

Chao, B. F., Y. H. Wu, and Y. S. Li (2008), Impact of artificial reservoir water impoundment on global sea level, *Science*, *320*, 212–214.

Chase, T. N., R. A. Pielke Sr., G. F. Kittel, R. R. Nemani, and S. W. Running (2000), Simulated impacts of historical land cover changes on global climate in northern winter. *Clim. Dyn.*, *16*, 93–105.

DeAngelis, A., F. Dominguez, Y. Fan, A. Robock, M. D. Kustu, and D. Robinson (2010), Evidence of enhanced precipitation due to irrigation over the Great Plains of the United States, *J. Geophys. Res*, *115*, D15115.

Degu, A. M., F. Hossain, D. Niyogi, R. Pielke Sr., J. M. Shepherd, N. Voisin, and T. Chronis (2011), The influence of large dams on surrounding climate and precipitation patterns, *Geophys. Res. Lett.*, *38*, L04405, doi:10.1029/2010GL046482.

Freydank, K., and S. Siebert (2008), *Towards mapping the extent of irrigation in the last century: A time series of irrigated area per country. Germany: Frankfurt Hydrology Paper 08*, Institute of Physical Geography, University of Frankfurt (Main).

Groisman, P. Y., et al. (1999), Changes in the probability of heavy precipitation: Important indicators of climatic change, *Clim. Change*, *42*(1), 243–283.

Groisman, P. Y., R. W. Knight, D. R. Easterling, T. R. Karl, G. C. Hegerl, and V. A. N. Razuvaev (2005), Trends in intense precipitation in the climate record, *J. Clim.*, *18*(9), 1326–1350.

GWSP (2008), Digital Water Atlas, Map 41: Dams and capacity of artificial reservoirs (V1.0), Bonn, Germany [Available at http://atlas.gwsp.org/]. AQ10

Hossain, F. (2010), On the empirical relationship between the presence of large dams the alteration in extreme precipitation, *Nat. Hazards Rev*, *11*, 97–101, doi:10.1061/(ASCE)NH.1527-6996.0000013. AQ4

Hossain, F., I. Jeyachandran, and R. A. Pielke Sr. (2010), Dam safety effects due to human alteration of extreme precipitation, *Water Resour. Res*, *46*, W03301. AQ5

Hossain, F., D. Niyogi, J. Adegoke, G. Kallos, and R. Pielke Sr. (2011), Making sense of the water resources that will be available in future use, *EOS Forum*, *92*(17). AQ6

Huffman, G. J., R. F. Adler, D. T. Bolvin, and E. J. Nelkin (2010), The TRMM multisatellite precipitation analysis (TMPA), in *Satellite Rainfall Applications for Surface Hydrology*, edited by M. Gebremichael and F. Hossain, pp. 3–22, Springer, New York.

Jacquot, J. (2009), Numbers dams, from Hoover to Three Gorges to the crumbling ones, *Discover Magazine*, March 2009, Last accessed online 24 May 2011, from http://discovermagazine.com/2009/mar/08-dams-hoover-three-gorges-crumbling-ones. AQ11

Jodar, J., J. Carrera, and A. Cruz (2010), Irrigation enhances precipitation at the mountains downwind, *Hydrol. Earth Syst. Sci.*, *7*, 3109–3127.

Lehner, B., and P. Döll (2004), Development and validation of a global database of lakes, reservoirs and wetlands, *J. Hydrol.*, *296*, 1–22.

Lehner, B., et al. (2011), High resolution mapping of the world's reservoirs and dams for sustainable river flow management, *Frontiers Ecol. Environ.*, in press. AQ7

Lempérière, F. (2006), The role of dams in XXI century: Achieving a sustainable development target, *Int. J. Hydropower Dams*, Issue 3, Last accessed online on 24 May 2011 from http://www.hydropower-dams.com/Issue-Three.php?c_id=60. AQ9

Moore, N., and S. Rojstaczer (2002), Irrigation's influence on precipitation: Texas High Plains, U.S.A., *Geophys. Res. Lett*, *29*(16), 1755.

Morin, E. (2011), To know what we cannot know: Global mapping of minimal detectable absolute trends in annual precipitation, *Water Resour. Res*, *47*, W07505.

Peel, M. C., B. L. Finlayson, and T. McMahon (2007), Updated world map of the Köppen–Geiger climate classification, *Hydrol. Earth Syst. Sci.*, *11*, 1633–1644.

Shepherd, J. M., H. Pierce, and A. J. Negri (2002), On rainfall modification by major urban areas: Observations from space-borne radar on TRMM, *J. Appl. Meteorol.*, *41*, 689–701.

Vörösmarty, C. J., and D. Sahagian (2000), Anthropogenic disturbance of the terrestrial water cycle, *Bioscience*, *50*(9). AQ8

A. M. Degu and F. Hossain, Department of Civil and Environmental Engineering, 1020 Stadium Dr., Box 5015, Cookeville, TN 38505-0001, USA. (fhossain@tntech.edu)